Structure and Stereochemistry in *f*-Block Complexes of High Co-ordination Number. Part 5.[1] Ten-co-ordination: The Crystal Structures of Tetrapotassium Tetraoxalatouranate(IV) Tetrahydrate(Orthorhombic and Triclinic Phases), Bicapped Square Antiprismatic and Sphenocoronal Stereochemistries †

Mark C. Favas, David L. Kepert, Jennifer M. Patrick, and Allan H. White
Department of Physical and Inorganic Chemistry, University of Western Australia, Nedlands, W.A. 6009

The title compond, $K_4[U(C_2O_4)_4]\cdot 4H_2O$, has been prepared in two crystalline modifications; the crystal structures of both have been determined by single-crystal *X*-ray diffraction methods at 295 K. One form is orthorhombic, space group *Fdd*2, with unit-cell dimensions $a = 30.09(2)$, $b = 22.18(1)$, $c = 12.747(6)$ Å, and $Z = 16$; $R = 0.043$ was obtained for 3 127 'observed' reflections; the other form is triclinic, space group $P\bar{1}$, with unit-cell dimensions $a = 9.595(5)$, $b = 12.998(4)$, $c = 10.329(5)$ Å, $\alpha = 115.47(3)$, $\beta = 80.49(4)$, $\gamma = 113.09(13)°$, and $Z = 2$; $R = 0.034$ for 6 017 independent reflections. In each case, the formula unit is the asymmetric unit; some disorder occurs among the cations in the orthorhombic phase. In both structures the uranium atom is ten-co-ordinate, one of the ligands in each case being bridging and linking the uranium atoms in an infinite one-dimensional polymeric array. For the orthorhombic phase U–O range between 2.37(1) and 2.58(1) Å, while in the triclinic form the range is 2.406(5)—2.641(4) Å. The co-ordination stereochemistries about the uranium atoms are examined in terms of a repulsion model.

In the previous paper[1] we examined further the system [M(bidentate ligand)$_4$] in regard to actinoid metal-atom stereochemistry and reported structure determinations of uranium(IV) and cerium(IV) dibenzoylmethanate complexes. Among other potential [M(bidentate ligand)$_4$] systems are the oxalate derivatives $[M(C_2O_4)_4]^{4-}$. Structure determinations carried out on $K_4[Zr,Hf(C_2O_4)_4]\cdot 5H_2O$[2,3] and $Na_4[Zr(C_2O_4)_4]\cdot 3H_2O$[4] show that in these complexes the metal is eight-co-ordinated by four bidentate oxalate ligands, with a D_{2d} dodecahedral stereochemistry. A report[5] of the structure determination of $K_4[Th(C_2O_4)_4]\cdot 4H_2O$ indicates the presence of ten-co-ordinate thorium(IV) with bidentate and bridging oxalate ligands, in a triclinic cell, and further states briefly that the uranium analogue is orthorhombic, space group *Fdd*2. In view of the comparable stoicheiometry with the zirconium, hafnium, and thorium analogues, and the new crystal type, we considered the possibility of a new stereochemical type sufficiently important to warrant investigation of the *Fdd*2 uranium oxalate complex. In synthesizing this, we also obtained a triclinic phase which proved to be isomorphous with the thorium structure. Structure determinations have therefore been carried out on both polymorphs of $K_4[U(C_2O_4)_4]\cdot 4H_2O$ and are compared with each other and with repulsion-theory predictions.

Experimental

The preparation of $K_4[U(C_2O_4)_4]\cdot 4H_2O$ has been reported a number of times, *e.g.* ref. 6.

In the present preparation, uranyl nitrate (1 g, 2.0 mmol) was dissolved in dilute hydrochloric acid (2 cm^3 concentrated HCl + 18 cm^3 water) and warmed to 80 °C. Sodium dithionite (0.75 g, 4.0 mmol) was added gradually with stirring followed by concentrated HCl (1 cm^3). The solution was heated to dissolve the solid, and then filtered to give a clear green solution. A solution of oxalic acid (0.45 g, 3.6 mmol) in water (5 cm^3) was slowly added with stirring, and the mixture stirred for another 30 min. The solid was washed five times by decantation (5 × 30 cm^3 water), filtered off, and air-dried, yielding $U(C_2O_4)_2\cdot 6H_2O$, 0.8 g (77%). This compound (0.4 g, 0.8 mmol) was placed in water (7 cm^3) and a solution of potassium oxalate (0.35 g, 1.9 mmol) in water (5 cm^3) added. The mixture was heated until all of the solid had dissolved. Crystals were obtained by adding a small amount of ethanol and allowing to stand, yielding both polymorphs.

Crystallography.—General procedural details are given in ref. 7.

Crystal data. Orthorhombic phase, $C_8H_8K_4O_{20}U$, $M = 818.6$, space group *Fdd*2 (C_{2v}^{19}, no. 43), $a = 30.09(2)$, $b = 22.18(1)$, $c = 12.747(6)$ Å, $U = 8\,504(7)$ Å^3, $D_m = 2.55(1)$, $Z = 16$, $D_c = 2.56$ g cm^{-3}, $F(000) = 6\,144$, $\mu_{Mo} = 82$ cm^{-1}. Specimen: hexagonal plate, thickness 0.08(*a*) × 0.17 × 0.255 mm; $2\theta_{max.} = 60°$, $N = 4\,028$, $N_o = 3\,127$, $R = 0.043$, $R' = 0.048$.

Triclinic phase, $C_8H_8K_4O_{20}U$, $M = 818.6$, space group $P\bar{1}$ (C_i^1, no. 2), $a = 9.595(5)$, $b = 12.998(4)$, $c = 10.329(5)$ Å, $\alpha = 115.47(3)$, $\beta = 80.49(4)$, $\gamma = 113.09(3)°$, $U = 1\,069(1)$ Å^3, $D_m = 2.55(1)$, $Z = 2$, $D_c = 2.54$ g cm^{-3}, $F(000) = 768$, $\mu_{Mo} = 81$ cm^{-1}. Crystal: irregular polyhedron, absorption correction modelled by spherical approximation, radius 0.15 cm; $2\theta_{max.} = 70°$, $N = 6\,779$, $N_o = 6\,017$, $R = 0.034$, $R' = 0.045$.

Abnormal features: orthorhombic phase. One of the cations was found to be disordered, the fragments being distinguished from those of the solvent molecules by consideration of difference maps and refinement behaviour as a function of

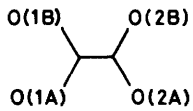

† *Supplementary data available* (No. SUP 23492, 37 pp.): thermal parameters, oxalate least-squares planes, structure factors. See Notices to Authors No. 7, *J. Chem. Soc., Dalton Trans.*, 1981, Index issue.

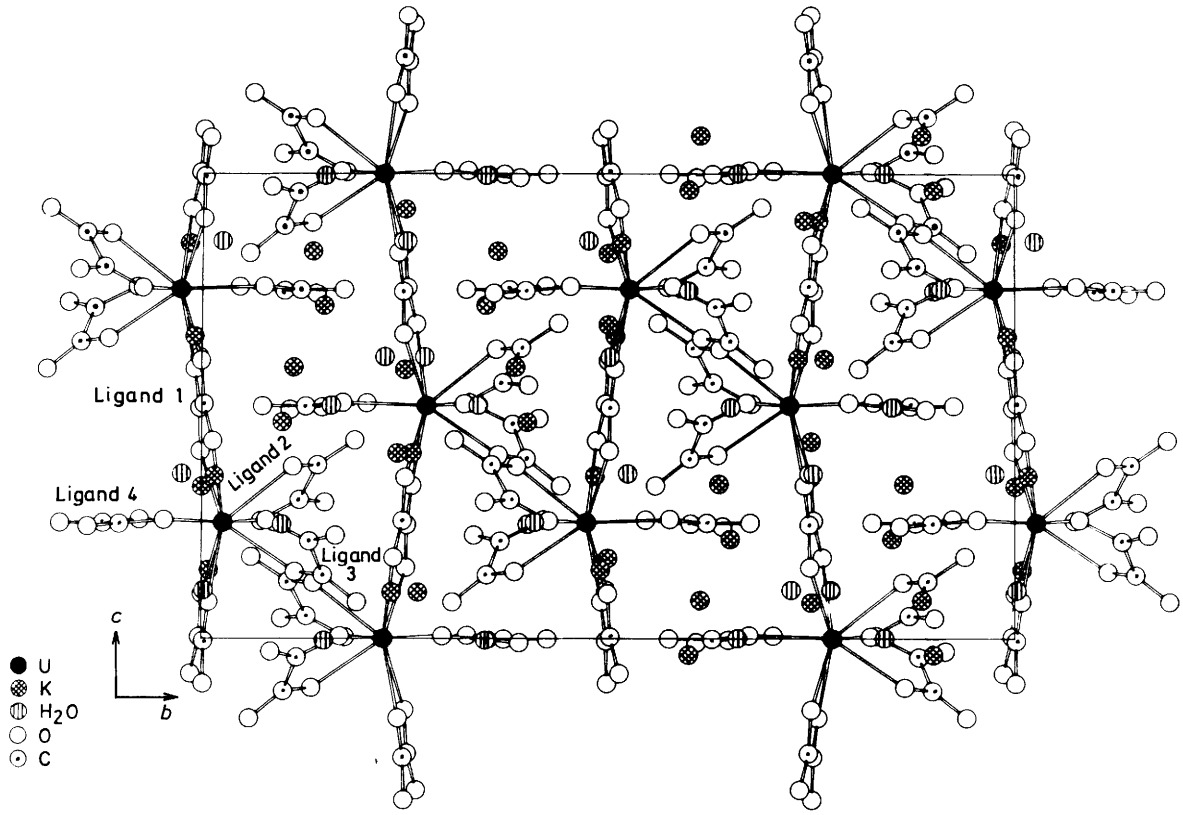

Figure 1. Unit-cell contents of the orthorhombic phase projected down *a* showing non-hydrogen atoms and ligand labelling. Only half the cell in *x* is shown

angular extent of the data; full-matrix least-squares refinement was used with fragment populations constrained to sum to 1, and with isotropic thermal parameters for the fragments. Oxalate numbering is as shown with the chelating oxygens in the non-bridging ligands being ' A '; ligand numbering is designed as far as possible to render comparable the co-ordination spheres of the uranium atoms. (The disposition of the centrosymmetric 1,1′ ligands in the triclinic phase does not allow full comparability.)

Triclinic phase. The cell setting follows that used in the study of the thorium analogue.

Discussion

Orthorhombic Phase.—Unit-cell contents are shown in projection in Figure 1; taking account of the presence of a disordered cation, the structure is consistent with the stoicheiometry $K_4[U(C_2O_4)_4]\cdot 4H_2O$, with one molecule comprising the asymmetric unit. In spite of the crystallographic uniqueness of the asymmetric unit, some difficulty was experienced initially in solving the structure because of the nature of the uranium atom site (see Table 1).

The structure comprises arrays of uranium atoms along *c*, each with three bidentate oxalate groups, and a fourth quadridentate oxalate bridging successive metal atoms, so that polymeric strings of $U(ox)_3$–ox–$U(ox)_3$–ox–$U(ox)_3$– arrays (ox = oxalate) are formed along *c*. The cations and water molecules lie in interstices between the chains. About the uranium (Figure 2), the oxalate groups chelate in the usual fashion by way of an oxygen atom from either end of the molecule, *cis* to the central bond (Table 2). About the potassium ions, oxalate and water oxygen atoms co-ordinate in

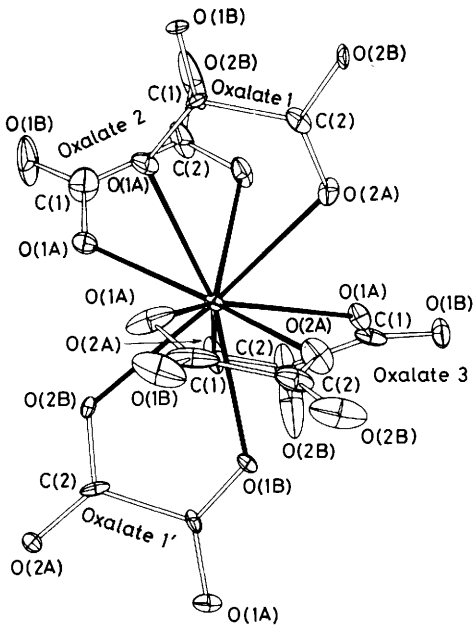

Figure 2. The uranium environment of the orthorhombic phase projected normal to the O_4 co-ordination plane of the bridging ligands

unsymmetrical arrays (Tables 3 and 4); we do not discuss the geometry of these further.

Table 1. Atom co-ordinates of the orthorhombic phase

Atom	*x*	*y*	*z*
(*a*) Cations			
K(1)	0.136 8(1)	0.234 0(2)	0.100 2(3)
K(2)	0.117 8(1)	0.009 0(1)	0.148 6(3)
K(3)	0.500 0(—)	0.000 0(—)	0.173 5(5)
K(4)	0.750 0(—)	0.250 0(—)	0.077 6(6)
K(5a) [a]	0.086 4(4)	0.099 4(5)	0.464 8(7)
K(5b) [b]	0.091 8(7)	0.113 6(9)	0.582 7(15)
(*b*) Anion			
U	0.256 31(1)	0.026 37(2)	0.250 00(—)
(*i*) Oxalate 1			
O(1A)	0.207 4(5)	−0.001 5(5)	0.403 5(9)
O(1B)	0.206 3(5)	−0.008 5(6)	0.579 5(9)
C(1)	0.224 4(4)	−0.002 4(6)	0.495 3(15)
C(2)	0.275 9(5)	0.002 8(7)	0.503 8(19)
O(2A)	0.298 6(4)	0.013 8(6)	0.424 9(10)
O(2B)	0.289 6(4)	−0.000 4(5)	0.596 8(9)
(*ii*) Oxalate 2			
O(1A)	0.183 1(3)	0.073 3(4)	0.254 0(9)
O(1B)	0.139 6(4)	0.151 7(7)	0.293 8(13)
C(1)	0.171 9(6)	0.120 6(7)	0.298 9(14)
C(2)	0.212 1(6)	0.143 1(7)	0.373 6(15)
O(2A)	0.247 3(3)	0.112 5(4)	0.370 7(8)
O(2B)	0.206 3(5)	0.188 8(9)	0.426 6(18)
(*iii*) Oxalate 3			
O(1A)	0.324 7(3)	0.079 6(3)	0.255 9(8)
O(1B)	0.360 5(3)	0.165 0(5)	0.222 7(7)
C(1)	0.328 9(5)	0.132 8(5)	0.210 0(8)
C(2)	0.289 9(5)	0.149 4(7)	0.137 3(15)
O(2A)	0.256 4(3)	0.115 0(4)	0.144 4(8)
O(2B)	0.294 1(5)	0.191 4(8)	0.079 0(15)
(*iv*) Oxalate 4			
O(1A)	0.235 1(5)	−0.076 4(4)	0.256 8(13)
O(1B)	0.252 4(6)	−0.175 0(4)	0.249 5(19)
C(1)	0.263 5(8)	−0.121 7(6)	0.248 9(19)
C(2)	0.313 7(6)	−0.101 6(7)	0.247 2(13)
O(2A)	0.317 9(4)	−0.046 4(4)	0.256 0(11)
O(2B)	0.342 0(6)	−0.140 9(5)	0.241 4(10)
(*c*) Water molecules			
O(1)	0.060 6(3)	0.090 3(5)	0.250 8(13)
O(2)	0.193 9(3)	0.150 9(5)	−0.003 6(10)
O(3)	0.106 9(5)	−0.002 6(5)	0.604 4(1)
O(4)	0.128 6(7)	0.225 6(13)	0.604 7(17)

[a] Population 0.45(1). [b] Population 1 − 0.45(1).

Table 2. Uranium environment of both phases: *r*(U–O) is the uranium–ligand distance (Å); the other entries in the matrix are the angles (°) subtended at the uranium by the two oxygen atoms at the head of the row and column

Orthorhombic	*r*(U–O)	O(12A)	O(21A)	O(22A)	O(31A)	O(32A)	O(41A)	O(42A)	O(11B^{i})	O(12B^{i})
O(11A)	2.52(1)	65.9(4)	64.0(4)	69.0(3)	127.1(4)	129.9(4)	65.1(5)	104.7(4)	154.8(4)	103.4(4)
O(12A)	2.58(1)		118.3(4)	66.4(4)	66.4(4)	125.2(4)	89.8(5)	62.1(4)	121.1(4)	159.5(4)
O(21A)	2.44(1)			63.7(3)	124.8(3)	70.2(3)	99.6(4)	163.9(3)	119.8(4)	67.0(4)
O(22A)	2.47(1)				72.0(3)	73.4(3)	133.8(5)	124.9(4)	136.1(4)	127.9(4)
O(31A)	2.37(1)					66.8(3)	135.3(4)	70.9(3)	73.4(4)	128.9(4)
O(32A)	2.38(1)						144.6(5)	123.9(4)	68.6(4)	75.3(4)
O(41A)	2.37(1)							64.5(4)	90.0(5)	69.7(5)
O(42A)	2.46(1)								65.2(4)	107.1(4)
O(11B^{i})	2.48(1)									61.4(4)
O(12B^{i})	2.46(1)									

Triclinic	*r*(U–O)	O(12A^{ii})	O(21A)	O(22A)	O(31A)	O(32A)	O(41A)	O(42A)	O(11B)	O(12B^{iii})
O(11A)	2.438(5)	63.2(2)	71.1(2)	76.4(2)	126.2(1)	142.9(2)	67.6(2)	83.1(2)	142.8(1)	112.6(2)
O(12A^{ii})	2.641(4)		116.5(2)	63.4(1)	63.4(2)	119.8(1)	109.9(1)	62.2(1)	116.4(2)	174.5(2)
O(21A)	2.429(5)			64.9(2)	130.0(1)	76.3(2)	89.1(2)	149.3(2)	126.7(1)	63.7(1)
O(22A)	2.429(5)				74.2(2)	74.1(2)	141.0(2)	125.4(1)	139.2(2)	120.0(1)
O(31A)	2.406(5)					65.5(1)	140.2(2)	78.7(1)	71.1(1)	121.1(1)
O(32A)	2.437(4)						129.6(1)	132.9(2)	72.4(1)	65.7(1)
O(41A)	2.444(5)							65.4(2)	79.4(2)	64.6(1)
O(42A)	2.432(4)								67.4(1)	114.6(1)
O(11B)	2.468(5)									64.4(1)
O(12B^{iii})	2.542(8)									

Transformations of the asymmetric unit: i $\frac{1}{2} - x, \bar{y}, z - \frac{1}{2}$; ii $\bar{x}, \bar{y}, \bar{z}$; iii $1 - x, 1 - y, \bar{z}$.

Triclinic Phase.—As expected the compound is isostructural with the thorium analogue; the structure of this has been discussed elsewhere.[5] Like the orthorhombic polymorph, the structure comprises an infinite polymer parallel to one of the crystallographic axes (*a* in this case), and the uranium atoms have three chelating oxalate groups and two others which chelate on both sides of the central C–C bond thus bridging adjacent uranium atoms (Figures 3 and 4). Unlike the orthorhombic form, in which the polymer is generated by a screw axis, the polymer in the triclinic phase is generated by a succession of inversion centres along *a*, located at the midpoints of the bridging oxalate C–C bonds. Successive units of the orthorhombic phase polymer are therefore of similar chirality, whereas successive units in the triclinic polymer are of opposite chirality; the crystal of the orthorhombic phase, nevertheless, is achiral, being a racemate of enantiomorphic polymer chains related by the mirror components of the space-group symmetry.

Table 3. Oxalate geometries for the orthorhombic phase; distances in Å, angles in degrees

	Oxalate ligand			
	1	2	3	4
C(1)–O(1A)	1.28(2)	1.24(2)	1.32(1)	1.32(2)
C(1)–O(1B)	1.21(2)	1.19(2)	1.20(2)	1.23(2)
C(1)–C(2)	1.56(2)	1.62(2)	1.54(2)	1.57(3)
C(2)–O(2A)	1.24(2)	1.26(2)	1.27(2)	1.24(2)
C(2)–O(2B)	1.26(3)	1.23(3)	1.20(3)	1.22(2)
O(1A) · · · O(2A)	2.78(2)	2.59(1)	2.62(1)	2.58(2)
O(1B) · · · O(2B)	2.52(2)	2.75(2)	2.77(2)	2.80(2)
U–O(1A)–C(1)	119(1)	128(1)	121(1)	124(1)
U–O(2A)–C(2)	117(1)	122(1)	123(1)	125(1)
O(1A)–C(1)–O(1B)	129(1)	133(2)	123(1)	124(2)
O(1A)–C(1)–C(2)	117(2)	109(1)	114(1)	114(1)
O(1B)–C(1)–C(2)	113(2)	118(2)	123(1)	122(2)
O(2B)–C(2)–C(1)	113(2)	118(2)	119(1)	118(1)
O(2A)–C(2)–C(1)	120(2)	116(1)	115(1)	112(1)
O(2A)–C(2)–O(2B)	127(1)	126(2)	127(1)	130(2)

parity in bond orders about each carbon atom as it is to chelation itself. In the bridging ligands, there is reasonable inverse correlation between U–O distance and C–O distance, the largest and shortest bond of each type being in correspondence. The non-bridging ligands, without the centrosymmetric constraints, are more or less distorted by torsion about the central C–C bond: for the planes of these ligands (2, 3, 4), σ (defining atoms) is 0.11, 0.24, and 0.25; for the oxalate planes in the orthorhombic phase, the maximum σ is 0.10 (ligand 3) with all others 0.03 or less.

The co-ordination polyhedra about the uranium atoms in both phases possess close to two-fold symmetry. The two most stable ten-co-ordinate polyhedra with two-fold symmetry are the bicapped square antiprism and the sphenocorona (or tetradecahedron) [6] (Figure 5). The former may be characterised by the two parallel square faces of the antiprism and an angle of 180° between the two bonds to the capping atoms. The sphenocorona may be characterised by the two planar trapezoidal faces meeting at an angle of approximately 102°. The relevant bond angles, dihedral angles,

Table 4. Potassium environments (K · · · O 3.5 Å) for the orthorhombic phase (presentation as for Table 2)

K(1)	*r*	O(31B^{i})	O(32B^{i})	O(12A^{ii})	O(31A^{ii})	O(42A^{ii})	
O(2)	2.84(1)	141.2(3)	83.4(4)	137.4(4)	82.5(3)	125.1(4)	
O(31B^{i})	2.73(1)		61.7(4)	79.7(3)	136.2(3)	81.9(3)	
O(32B^{i})	2.67(2)			139.1(5)	147.0(5)	103.2(4)	
O(12A^{ii})	2.82(1)				59.7(3)	55.4(3)	
O(31A^{ii})	2.63(1)					62.5(3)	
O(42A^{ii})	2.77(1)						
K(2)	***r***	**O(1)**	**O(12B^{iii})**	**O(21B^{iv})**	**O(22B^{iv})**	**O(4^{iv})**	**O(31B^{ii})**
O(21A)	2.77(1)	83.1(3)	57.1(3)	137.7(3)	143.6(5)	69.2(6)	97.7(3)
O(1)	2.81(1)		138.0(3)	137.2(4)	78.9(5)	75.7(6)	86.4(4)
O(12B^{iii})	2.87(1)			84.7(4)	141.3(5)	99.4(5)	86.1(3)
O(21B^{iv})	2.74(2)				60.3(5)	103.6(7)	97.2(4)
O(22B^{iv})	2.74(2)					75.7(7)	112.4(5)
O(4^{iv})	2.73(2)						158.8(6)
O(31B^{ii})	2.81(1)						
K(3)	***r***	**O(32B^{vi})**	**O(2^{iv})**	**O(32B^{vii})**	**O(2^{vii})**	**O(41B^{viii})**	
O(41B^{v})	2.77(2)	149.0(5)	136.1(5)	108.0(5)	77.8(4)	73.8(5)	
O(32B^{vi})	2.72(2)		72.0(4)	86.3(6)	81.1(4)	108.0(5)	
O(2^{vi})	2.92(1)			81.1(4)	142.9(4)	77.8(4)	
O(32B^{vii})	2.72(2)				72.0(4)	149.0(5)	
O(2^{vii})	2.92(1)					136.1(5)	
O(41B^{viii})	2.77(2)						
K(4)	***r***	**O(41B^{x})**	**O(41B^{xi})**	**O(22B^{xii})**	**O(1^{v})**	**O(1^{xiii})**	
O(22B^{ix})	2.70(2)	152.3(5)	104.5(6)	89.0(6)	78.4(5)	73.5(4)	
O(41B^{x})	2.75(2)		74.5(5)	104.5(6)	82.3(5)	132.4(5)	
O(41B^{xi})	2.75(2)			152.3(5)	132.4(5)	82.3(4)	
O(22B^{xii})	2.70(2)				73.5(4)	78.4(5)	
O(1^{v})	2.88(1)					140.2(5)	
O(1^{xiii})	2.88(1)						

Transformations of the asymmetric unit: i $\frac{1}{2} - x, \frac{1}{2} - y, z$; ii $x - \frac{1}{4}, \frac{1}{4} - y, z - \frac{1}{4}$; iii $\frac{1}{2} - x, \bar{y}, z - \frac{1}{2}$; iv $\frac{1}{4} - x, y - \frac{1}{4}, z - \frac{1}{4}$; v $\frac{3}{4} - x, y + \frac{1}{4}, z - \frac{1}{4}$; vi $\frac{3}{4} - x, y - \frac{1}{4}, \frac{1}{4} + z$; vii $\frac{1}{4} + x, \frac{1}{4} - y, \frac{1}{4} + z$; viii $\frac{1}{4} + x, y - \frac{1}{4}, z - \frac{1}{4}$; ix $\frac{1}{2} + x, y, z - \frac{1}{2}$; x $\frac{1}{2} + x, \frac{1}{2} + y, z$; xi $1 - x, \bar{y}, z$; xii $1 - x, \frac{1}{2} - y, z - \frac{1}{2}$; xiii $\frac{3}{4} + x, \frac{1}{4} - y, z - \frac{1}{4}$.

The structure determination of the triclinic phase (Tables 5—7) is of superior precision to that of the orthorhombic phase, sufficient to be able confidently to conclude that, as expected, the co-ordinated O–C bonds of the non-bridging ligands are longer than the non-co-ordinated, and that the O · · · O distance across the chelate is less than the O · · · O distance [O(B) · · · O(A)] between the non-co-ordinating oxygen atoms (2.6_2 *cf.* 2.8 Å). This is presumably at least as much a consequence of angular distortion due to the dis- and deviations from least-squares planes calculated from the atomic co-ordinates of the orthorhombic and triclinic phases are collected in Table 8. The co-ordination polyhedron in the triclinic phase is quite well described as a bicapped square antiprism with O(12A) and O(12B) as the capping sites [deviations from the least-squares planes of the 'square' faces 0.01—0.03 Å, vertex angles in the 'square' faces 84—96°, edge lengths of the 'squares' 2.90—3.42 Å, dihedral angle between the 'square' faces 4.4°, and an O(12A)–

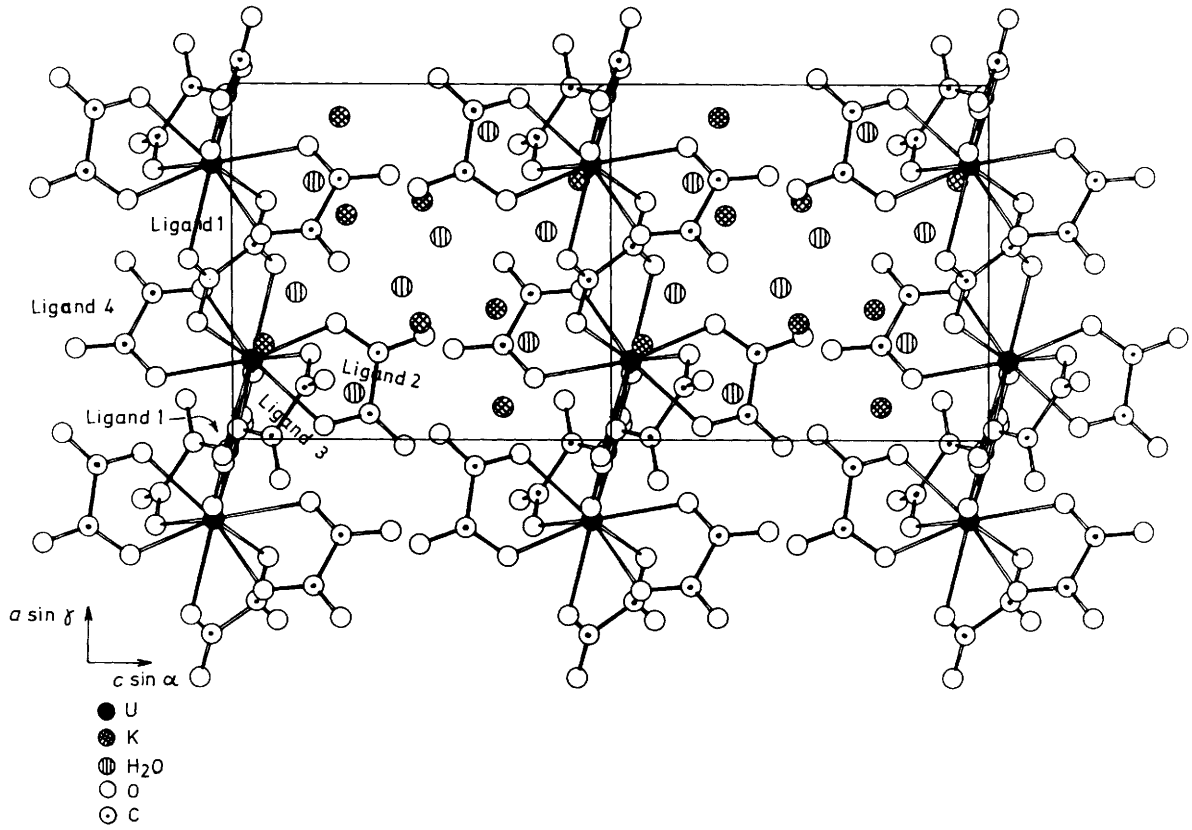

Figure 3. Unit-cell contents of the triclinic phase projected down *a*

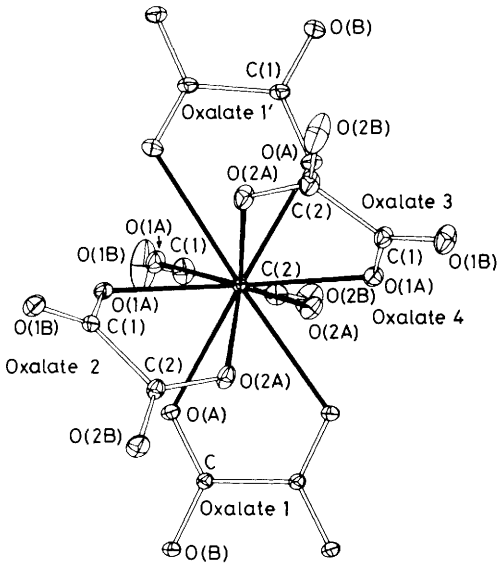

Figure 4. The uranium environment in the triclinic phase, projected similarly to Figure 2 (in each case 20% thermal ellipsoids are shown)

U–O(12B) angle of 175°]. A sphenocoronal description is less satisfactory (deviations from least-squares planes of the 'trapezoidal' faces 0.17—0.28 Å, sets of 'equivalent' trapezoidal vertex angles of 72—105 and 72—102°, and 'equivalent' trapezoidal edge lengths of 2.63—2.72 Å).

In the orthorhombic phase there are two alternative orientations of a bicapped square antiprism which can be considered, with either O(11A) and O(11B) or O(12A) and O(12B) as the

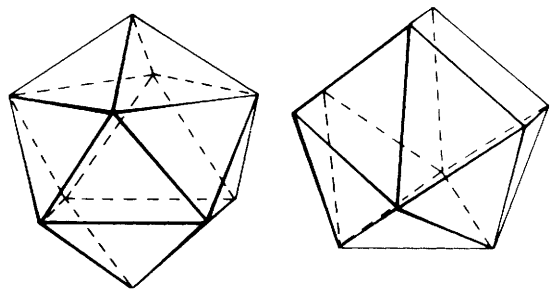

Figure 5. Bicapped square antiprism and sphenocorona

capping atoms. Neither is very satisfactory however, the deviations from ideality being much greater than those in the triclinic case (Table 8). On the other hand the sphenocoronal description is better for this phase than for the triclinic phase (deviations from least-squares planes of the trapezoidal faces of 0.11—0.13 Å, sets of 'equivalent' trapezoidal vertex angles of 82—98° for the four angles made to the edge common to both trapezoids and 81—100° for the other four angles, and 'equivalent' trapezoidal edge lengths of 2.60—2.76 Å).

An alternative procedure for determining the co-ordination polyhedra consists of considering the stereochemistry described by the points where the metal–ligand bonds cut a sphere of unit radius about the metal atom, and averaging the structure about a two-fold axis. Using this procedure the sphenocoronal description of the orthorhombic form is substantially improved (sets of 'equivalent' trapezoidal vertex angles of 89 and 89 for the two independent angles made to the edge common to both trapezoids and 90 and 91° for the other two independent angles, 'equivalent' trapezoidal

Table 5. Atom co-ordinates for the triclinic phase

Atom	*x*	*y*	*z*
(*a*) Cations			
K(1)	0.268 4(2)	0.799 5(2)	0.083 0(2)
K(2)	0.907 3(1)	0.693 2(1)	0.285 9(1)
K(3)	0.631 9(2)	0.394 7(2)	0.303 2(2)
K(4)	0.671 7(2)	0.161 2(1)	0.503 6(2)
(*b*) Anion			
U	0.223 69(2)	0.279 82(1)	0.051 97(2)
(*i*) Oxalate 1			
O(1A)	0.188 4(4)	0.084 5(4)	0.054 7(5)
O(1B)	0.045 0(5)	−0.105 3(4)	0.027 7(5)
C	0.066 3(5)	−0.007 0(5)	0.023 9(6)
(*ii*) Oxalate 1′			
O(1A)	0.329 6(4)	0.403 4(3)	−0.091 9(4)
O(1B)	0.506 8(4)	0.568 0(3)	0.115 0(4)
C	0.452 6(5)	0.491 9(4)	−0.059 6(5)
(*iii*) Oxalate 2			
O(1A)	0.326 0(4)	0.317 3(5)	0.274 7(4)
O(1B)	0.292 3(5)	0.354 9(5)	0.507 5(4)
C(1)	0.245 4(6)	0.319 9(5)	0.385 4(6)
C(2)	0.073 3(6)	0.275 8(7)	0.361 2(6)
O(2A)	0.039 3(4)	0.264 4(5)	0.240 9(4)
O(2B)	−0.016 3(6)	0.255 9(8)	0.453 5(6)
(*iv*) Oxalate 3			
O(1A)	0.029 4(4)	0.337 0(3)	0.012 7(4)
O(1B)	−0.112 1(4)	0.451 3(4)	0.123 6(5)
C(1)	0.008 5(5)	0.434 2(5)	0.103 4(5)
C(2)	0.150 5(5)	0.533 0(5)	0.193 5(5)
O(2A)	0.241 7(4)	0.488 5(4)	0.207 1(5)
O(2B)	0.168 2(5)	0.642 2(4)	0.242 9(5)
(*v*) Oxalate 4			
O(1A)	0.422 7(4)	0.202 1(4)	−0.078 4(4)
O(1B)	0.499 5(5)	0.083 5(5)	−0.282 6(5)
C(1)	0.410 0(6)	0.133 0(5)	−0.211 2(6)
C(2)	0.267 9(7)	0.112 1(6)	−0.284 8(6)
O(2A)	0.175 3(4)	0.157 9(4)	−0.203 3(4)
O(2B)	0.254 5(8)	0.054 9(8)	−0.416 1(6)
(*c*) Water molecules			
O(1)	0.131 0(6)	0.927 8(5)	0.322 1(6)
O(2)	0.724 3(7)	0.201 3(6)	0.218 1(7)
O(3)	0.429 4(6)	0.654 1(5)	0.448 3(6)
O(4)	0.414 3(15)	0.071 5(13)	0.172 2(15)

Table 6. Oxalate geometries for the triclinic phase

	Oxalate ligand				
	1	1′	2	3	4
C(1)–O(1A)	1.262(5)	1.251(5)	1.265(7)	1.277(6)	1.270(6)
C(1)–O(1B)	1.230(9)	1.249(8)	1.238(8)	1.230(8)	1.230(9)
C–C	1.538(9)	1.544(8)	1.546(8)	1.546(6)	1.545(11)
C(2)–O(2A)			1.269(9)	1.276(9)	1.260(8)
C(2)–O(2B)			1.217(9)	1.233(8)	1.235(8)
O(1A) · · · O(2A)	2.667(8)	2.672(7)	2.606(6)	2.620(5)	2.633(7)
O(1B) · · · O(2B)			2.770(7)	2.853(5)	2.741(11)
U–O(1A)–C(1)	125.0(5)	121.7(4)	122.3(4)	120.5(3)	121.6(4)
U–O(2A)–C(2)	117.9(4)	119.1(3)	122.8(4)	121.3(3)	122.0(4)
O(1A)–C(1)–O(1B)	126.1(7)	126.4(6)	126.1(6)	125.4(4)	125.8(7)
O(1A)–C(1)–C(2)	116.2(6)	116.8(5)	114.9(5)	114.0(5)	115.0(6)
O(1B)–C(1)–C(2)	117.7(4)	116.9(4)	118.9(7)	120.6(4)	119.2(5)
O(2B)–C(2)–C(1)			120.4(7)	120.8(6)	118.7(7)
O(2A)–C(2)–C(1)			113.9(7)	113.0(5)	115.9(5)
O(2A)–C(2)–O(2B)			125.7(6)	126.3(5)	125.4(8)

edge lengths of 1.07 and 1.08 times the unit radius), but there is no marked improvement in any of the other polyhedral descriptions listed in Table 8.

Whether the co-ordination polyhedron of the orthorhombic phase is best described as a sphenocorona or as either of the bicapped square antiprisms depends upon which criterion is taken to be the most important. Certainly it has undergone significant distortion from the bicapped square antiprism of the triclinic phase towards a sphenocorona (see below).

Repulsion-energy Calculations.—[M(unidentate ligand)$_{10}$]. There is as yet no structurally characterised ten-co-ordinate compound containing ten unidentate ligands. Nevertheless, the geometry of these hypothetical compounds is a useful introduction to the stereochemistry of [M(bidentate ligand)$_5$].

There are two semiregular and five non-uniform polyhedra with ten vertices.[8] An additional convex polyhedron is created if the tetracapped trigonal prism, in which the three square faces and one triangular face of the prism are capped, is distorted so that all vertices lie on the surface of a sphere. Minimisation of the total repulsion energy [6] and/or placing all atoms on the surface of a sphere leads to distortion in all cases and to two of the polyhedra becoming identical. The repulsion-energy coefficients, X, calculated for $n = 6$, are listed in Table 9 for the remaining structures.[6,9,10]

The first three structures are substantially more stable than the other four. The differences in energy among these three polyhedra are small and all three stereochemistries, or intermediates lying along various reaction co-ordinates connecting them, would be possible. The pentagonal antiprism and pentagonal prism are among the less stable ten-co-ordinate polyhedra, but they do allow the positioning of five equivalent bidentate ligands, and hence are of relevance to [M(bidentate ligand)$_5$].

[M(bidentate ligand)$_5$]. *The theoretical stereochemistries.* Five distinct stereochemistries exist as minima on the potential-energy surfaces calculated for [M(bidentate ligand)$_5$] over a range of normalised bite, b, all of which show some relation-

Table 7. Potassium environments (K · · · O 3.5 Å) for the triclinic phase (presentation as for Table 2)

K(1)	r(K · · · O)	O(1)	O(4^{I})	O(41A^{II})	O(41B^{II})	O(2^{II})	O(11B^{I})	O(31A^{III})	O(31B^{III})
O(32B)	2.945(6)	77.7(2)	133.2(3)	88.2(2)	79.2(2)	143.7(2)	119.9(1)	79.1(1)	73.1(1)
O(1)	2.779(6)		67.6(3)	125.1(2)	79.6(2)	124.7(2)	63.2(2)	82.9(1)	124.1(1)
O(4^{I})	3.009(15)			87.1(3)	64.8(4)	83.0(3)	70.8(3)	124.2(4)	153.2(4)
O(41A^{II})	2.965(5)				45.5(1)	97.4(2)	151.5(1)	146.2(1)	100.7(1)
O(41B^{II})	2.773(6)					128.8(2)	130.3(2)	154.5(2)	137.0(2)
O(2^{II})	3.095(8)						63.2(2)	76.5(1)	70.6(2)
O(11B^{I})	3.089(6)							53.6(1)	92.4(1)
O(31A^{III})	2.782(4)								45.7(1)
O(31B^{III})	2.945(4)								

K(2)	r(K · · · O)	O(32B^{IV})	O(1^{IV})	O(22B^{V})	O(21B^{V})	O(1′1A^{II})	O(31A^{II})	O(42A^{II})
O(31B^{IV})	2.800(5)	61.8(1)	134.8(2)	102.7(3)	95.7(2)	75.9(1)	72.4(1)	128.0(1)
O(32B^{IV})	2.754(6)		79.5(2)	70.5(2)	119.4(2)	128.4(1)	79.9(1)	131.7(1)
O(1^{IV})	2.863(6)			83.9(2)	124.8(2)	117.4(2)	78.9(1)	63.0(2)
O(22B^{V})	2.763(8)				60.5(2)	151.9(2)	148.0(1)	129.3(2)
O(21B^{V})	2.734(5)					91.4(1)	150.0(1)	107.1(2)
O(1′1A^{II})	2.804(5)						59.2(1)	57.8(1)
O(31A^{II})	2.926(4)							64.5(1)
O(42A^{II})	2.819(6)							

K(3)	r(K · · · O)	O(21A)	O(2)	O(31B^{IV})	O(21B^{V})	O(3^{V})
O(1′1B^{II})	2.820(6)	56.4(1)	122.9(2)	81.3(2)	89.9(2)	141.0(2)
O(21A)	2.726(4)		111.0(2)	134.8(2)	102.5(1)	86.6(2)
O(2)	2.733(9)			77.0(2)	142.2(2)	79.1(2)
O(31B^{IV})	2.875(5)				91.7(1)	137.6(2)
O(21B^{V})	2.843(6)					86.3(2)
O(3^{V})	2.819(8)					

K(4)	r(K · · · O)	O(41B^{VI})	O(32B^{V})	O(3^{V})	O(42B^{VII})	O(41B^{VII})
O(22B^{IV})	2.809(6)	133.8(2)	68.2(1)	104.6(3)	79.9(3)	115.5(2)
O(41B^{VI})	2.834(6)		79.5(1)	98.2(2)	83.6(2)	88.5(2)
O(32B^{V})	2.871(4)			75.9(2)	113.0(2)	164.6(2)
O(3^{V})	2.756(8)				171.2(2)	115.7(2)
O(42B^{VII})	2.893(11)					55.5(2)
O(41B^{VII})	2.987(5)					

Transformations of the asymmetric unit: i x, $1 + y$, z; ii $1 - x$, $1 - y$, $\bar{z}$; iii $\bar{x}$, $1 - y$, $\bar{z}$; iv $1 + x$, y, z; v $1 - x$, $1 - y$, $1 - z$; vi x, y $1 + z$; vii $1 - x$, $\bar{y}$, $\bar{z}$.

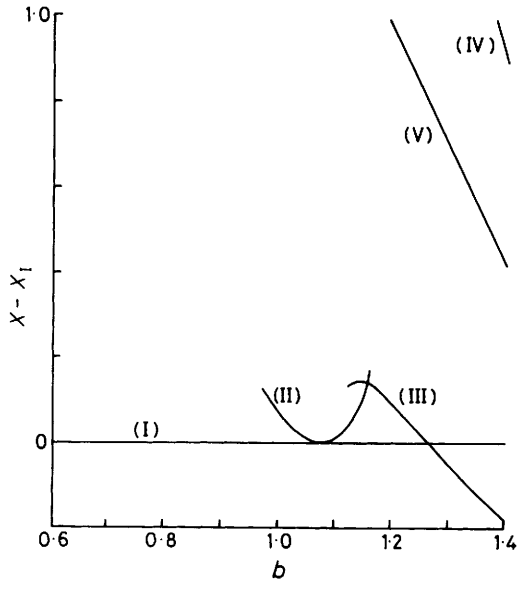

Figure 6. Repulsion-energy coefficients, X, relative to those for isomer (I), for the various isomers of [M(bidentate ligand)$_5$], and as a function of b; $n = 6$

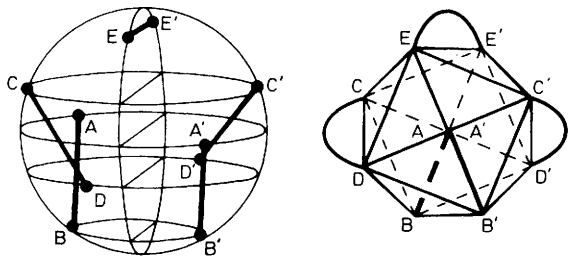

Figure 7. Isomer (I) for [M(bidentate ligand)$_5$]; $b = 1.085$, $n = 6$

ship to the structures calculated for [M(unidentate ligand)$_{10}$].

The differences among the repulsion-energy coefficients are shown in Figure 6. Isomers (IV) and (V) have prohibitively high repulsion energies and will not be considered further.

Isomer (I), Figure 7, contains a two-fold axis and approximates a bicapped square antiprism. The two bidentate ligands with atoms at the capping sites have their other ends on two adjacent vertices of the square antiprism, and this structure can accordingly be called the *cis* isomer. The remaining three bidentate ligands form a three-bladed propeller. As the normalised bite is reduced, the two square faces rotate towards one another.

Isomer (II) (Figure 8) also contains a two-fold axis and is

Table 8. Structural parameters for triclinic and orthorhombic phases; distances in Å, angles in degrees

(*a*) Triclinic: bicapped square antiprism, O(12A) and O(12B) as capping atoms

Plane atom	O(11A)	O(42A)	O(31A)	O(22A)
Deviation	0.01	−0.01	0.01	−0.01
Vertex angle	87.5	86.6	92.3	93.5
Edge length	O(11A)–O(42A)	O(42A)–O(31A)	O(31A)–O(22A)	O(22A)–O(11A)
	3.23	3.07	2.92	3.01
Plane atoms	O(11B)	O(41A)	O(21A)	O(32A)
Deviation	0.02	−0.02	0.02	−0.03
Vertex angle	93.9	83.7	86.7	95.7
Edge length	O(11B)–O(41A)	O(41A)–O(21A)	O(21A)–O(32A)	O(32A)–O(11B)
	3.14	3.42	3.01	2.90

Dihedral angle between planes = 4.4°; O(12A)UO(12B) = 174.5°

(*b*) Triclinic: sphenocorona

Plane atom	O(11A)	O(12A)	O(42A)	O(41A)
Deviation	−0.17	0.18	−0.19	0.18
Vertex angle	101.4	75.2	104.8	74.2
Edge length	O(11A)–O(12A)	O(12A)–O(42A)	O(42A)–O(41A)	O(41A)–O(11A)
	2.67	2.63	2.62	2.72
Plane atom	O(41A)	O(42A)	O(11B)	O(12B)
Deviation	−0.28	0.27	−0.27	0.27
Vertex angle	104.4	71.8	101.9	72.0
Edge length	O(41A)–O(42A)	O(42A)–O(11B)	O(11B)–O(12B)	O(12B)–O(41A)
	2.63	2.72	2.67	2.67

Dihedral angle between planes = 105.3°

(*c*) Orthorhombic: bicapped square antiprism, O(11A) and O(11B) as capping atoms

Plane atom	O(12A)	O(41A)	O(21A)	O(22A)
Deviation	−0.07	0.05	−0.07	0.09
Vertex angle	89.7	73.8	88.9	107.1
Edge length	O(12A)–O(41A)	O(41A)–O(21A)	O(21A)–O(22A)	O(22A)–O(12A)
	3.50	3.67	2.59	2.76
Plane atom	O(12B)	O(42A)	O(31A)	O(32A)
Deviation	−0.02	0.03	−0.04	0.04
Vertex angle	74.8	78.3	104.0	102.8
Edge length	O(12B)–O(42A)	O(42A)–O(31A)	O(31A)–O(32A)	O(32A)–O(12B)
	3.96	2.80	2.62	2.96

Dihedral angle between planes = 17.4°; O(11A)UO(11B) = 154.8°

(*d*) Orthorhombic: bicapped square antiprism, O(12A) and O(12B) as capping atoms

Plane atom	O(42A)	O(31A)	O(22A)	O(11A)
Deviation	0.03	−0.04	0.04	−0.03
Vertex angle	79.0	101.3	101.2	78.4
Edge length	O(42A)–O(31A)	O(31A)–O(22A)	O(22A)–O(11A)	O(11A)–O(42A)
	2.80	2.85	2.83	3.95
Plane atom	O(41A)	O(21A)	O(32A)	O(11B)
Deviation	0.14	−0.18	0.23	−0.20
Vertex angle	73.5	88.1	101.0	93.7
Edge length	O(41A)–O(21A)	O(21A)–O(32A)	O(32A)–O(11B)	O(11B)–O(41A)
	3.67	2.77	2.74	3.43

Dihedral angles between planes = 16.8°; O(12A)UO(12B) = 159.5°

(*e*) Orthorhombic: sphenocorona

Plane atom	O(11B)	O(12B)	O(41A)	O(42A)
Deviation	−0.13	0.13	−0.12	0.13
Vertex angle	99.5	80.9	95.6	81.8
Edge length	O(11B)–O(12B)	O(12B)–O(41A)	O(41A)–O(42A)	O(42A)–O(11B)
	2.52	2.76	2.58	2.66
Plane atom	O(41A)	O(42A)	O(12A)	O(11A)
Deviation	−0.12	0.12	−0.11	0.11
Vertex angle	98.4	85.0	94.4	80.5
Edge length	O(41A)–O(42A)	O(42A)–O(12A)	O(12A)–O(11A)	O(11A)–O(41A)
	2.58	2.60	2.78	2.64

Dihedral angle between planes = 105.8°

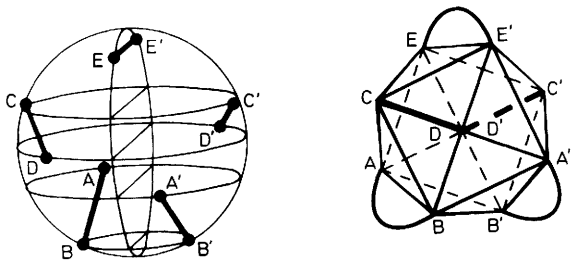

Figure 8. Isomer (II) for [M(bidentate ligand)$_5$]; b = 1.085, n = 6

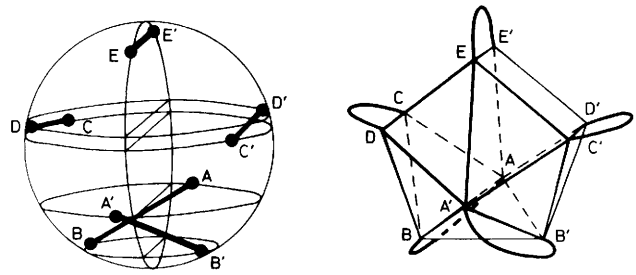

Figure 9. Isomer (III) for [M(bidentate ligand)$_5$]; b = 1.13, n = 6

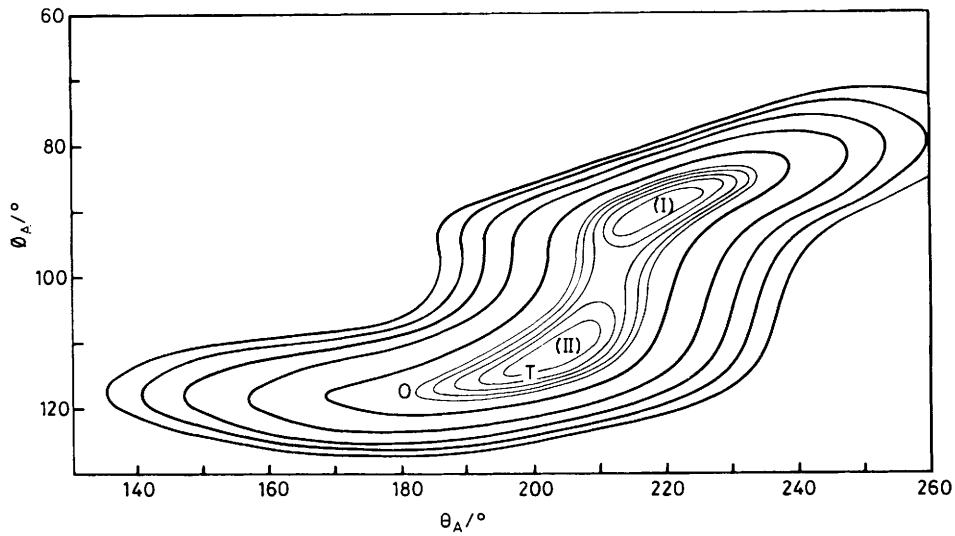

Figure 10. Projection of the potential-energy surface for [M(bidentate ligand)$_5$] onto the φ_A–θ_A plane. The five faint contour lines are for successive 0.02 increments above the minimum and the five heavy contour lines for successive 0.2 increments above the minimum; n = 6, b = 1.07. The positions of isomers (I) and (II) and the orthorhombic (O) and triclinic (T) phases are marked

Table 9. Repulsion-energy coefficients for [M(unidentate ligand)$_{10}$] (n = 6)

Stereochemistry	X
Bicapped square antiprism	12.337
Sphenocorona	12.362
Tetracapped trigonal prism	12.363
Pentagonal antiprism	14.637
Bicapped cube	15.375
Pentagonal prism	15.522
Capped tridiminished icosahedron	21.692

closely related to a bicapped square antiprism. However, the two bidentate ligands attached to the capping atoms now have their other ends attached to two nearly opposite vertices of the antiprism, and hence this structure can be termed the *trans* isomer. Of the remaining bidentate ligands, one is twisted in the opposite direction to the other two when viewed down the four-fold axis of the antiprism, and thus variation of the normalised bite cannot be accommodated by rotation of the square faces of the antiprism relative to each other. Isomer (II) exists as a separate minimum only over the range 0.97 $\leqslant b \leqslant$ 1.16 (for n = 6).

Isomer (III) (Figure 9) again contains a two-fold axis and is based upon the sphenocorona structure of [M(unidentate ligand)$_{10}$]. It exists as a minimum on the potential-energy surface only for $b \geqslant$ 1.13 (for n = 6).

The relationship between these three important stereochemistries is shown by the potential-energy surfaces in Figures 10 and 11 (φ is equivalent to the latitude of a point on the surface of a sphere relative to a North pole, and θ is equivalent to the longitude). The surface for b = 1.2 (Figure 11) shows only the presence of isomers (I) and (III), whereas at b = 1.07 (Figure 10) (as in the present compounds) isomers (I) and (II) exist as minima. The positions of the triclinic and orthorhombic phases are marked.

Comparison with experiment. Table 10 contains the known compounds of the type [M(bidentate ligand)$_5$]. The angular parameters have been averaged assuming a two-fold axis, although a crystallographic two-fold axis is present only in $[PEtPh_3]_2[Ce(NO_3)_5]$ and $[AsPh_4]_2[Eu(NO_3)_5]$. The orthorhombic phase of $K_4[U(C_2O_4)_4]\cdot 4H_2O$ shows the greatest deviation from two-fold symmetry, the average angular difference subtended at the metal atom between an atom and its two-fold average position being 8.6°. The triclinic phase had a very much better two-fold axis.

All compounds listed in Table 10 with four-membered nitrate or carbonate chelate rings have normalised bites in the range 0.8—0.9 and are all of stereochemistry (I) as predicted from the calculations. The agreement between observed and calculated angular parameters is quite reasonable (Table 10: the experimental polyhedron has been rotated about the two-fold axis relative to the calculated polyhedron to minimise the distance between the calculated and experimental atom sites). The average angular difference, δ, between the calculated and observed atom sites, given as the angle subtended at the cen-

Table 10. Structural parameters for [M(bidentate ligand)$_5$]

Compound	Isomer	*b*(av.)	φ_A/°		θ_A/°		φ_B/°		θ_B/°		φ_C/°		θ_C/°		φ_D/°		θ_D/°		φ_E/°		θ_E/°		δ/°	Ref.
			Obs.	Calc.	Obs.	Calc.	Obs.	Calc.	Obs.	Calc.	Obs.	Calc.	Obs.	Calc.	Obs.	Calc.	Obs.	Calc.	Obs.	Calc.	Obs.	Calc.		
$[PEtPh_3]_2[Ce(NO_3)_5]$	(I)	0.84	95	96	204	204	144	143	219	223	75	74	275	274	110	106	310	312	25	25	12	0	3	*a*
$[AsPh_4]_2[Eu(NO_3)_5]$	(I)	0.87	95	95	206	206	142	144	231	227	76	73	272	274	104	107	315	314	26	26	−1	0	2	*b*
$K_2[Er(NO_3)_5]$	(I)	0.88	95	95	206	206	145	144	217	228	73	73	275	275	107	107	314	315	26	26	8	0	2	*c*
$[NO]_2[Ho(NO_3)_5]$	(I)	0.88	96	95	206	206	145	144	220	228	74	73	276	275	107	107	314	315	27	26	9	0	3	*d*
$Na_6[Th(CO_3)_5]\cdot 12H_2O$	(I)	0.88	95	95	206	206	144	144	219	228	72	73	274	275	102	107	314	315	26	26	3	0	3	*e*
$Na_6[Ce(CO_3)_5]\cdot 12H_2O$	(I)	0.89	94	95	207	207	145	144	220	229	71	73	274	275	103	107	315	316	26	26	4	0	3	*f*
$[C(NH_2)_3]_6[Th(CO_3)_5]\cdot 4H_2O$	(I)	0.88	92	95	204	206	141	144	223	228	75	73	276	275	111	107	315	315	26	26	4	0	3	*g*
$[C(NH_2)_3]_6[Ce(CO_3)_5]\cdot 4H_2O$	(I)	0.90	92	94	205	207	142	144	224	231	74	72	276	275	110	107	317	317	27	27	4	0	3	*h*
$[Ba(MeCONHCOMe)_5][ClO_4]_2$	(II)	0.98	104	111	210	202	147	146	262	267	68	71	263	261	96	90	316	317	30	29	−6	0	5	*i*
$K_4[Th(C_2O_4)_4]\cdot 4H_2O$ (triclinic)	(II)	1.05	116	111	201	204	142	146	281	278	71	70	258	258	88	90	320	320	32	32	1	0	3	5
$K_4[U(C_2O_4)_4]\cdot 4H_2O$ (triclinic)	(II)	1.07	115	111	201	205	143	146	282	280	71	70	258	258	88	90	321	321	33	32	1	0	3	This work
(orthorhombic)	(II)–(III)	1.07	117	111	199	205	143	146	283	280	80	70	257	258	81	90	321	321	32	32	19	0	8	This work

[a] A. R. Al-Karaghouli and J. S. Wood, *J. Chem. Soc., Dalton Trans.*, 1973, 2318. [b] J.-C. G. Bunzli, B. Klein, G. Chapuis, and K. J. Schenk, *J. Inorg. Nucl. Chem.*, 1980, **42**, 1307. [c] E. G. Sherry, *J. Inorg. Nucl. Chem.*, 1978, **40**, 257. [d] G. E. Toogood and C. Chieh, *Can. J. Chem.*, 1975, **53**, 831. [e] S. Voliotis and A. Rimsky, *Acta Crystallogr., Sect. B*, 1975, **31**, 2615. [f] S. Voliotis and A. Rimsky, *Acta Crystallogr., Sect. B*, 1975, **31**, 2620. [g] S. Voliotis and A. Rimsky, *Acta Crystallogr., Sect. B*, 1975, **31**, 2612. [h] S. Voliotis, A. Rimsky, and J. Faucherre, *Acta Crystallogr., Sect. B*, 1975, **31**, 2607. [i] P. S. Gentile, J. White, and S. Haddad, *Inorg. Chim. Acta*, 1975, **13**, 149.

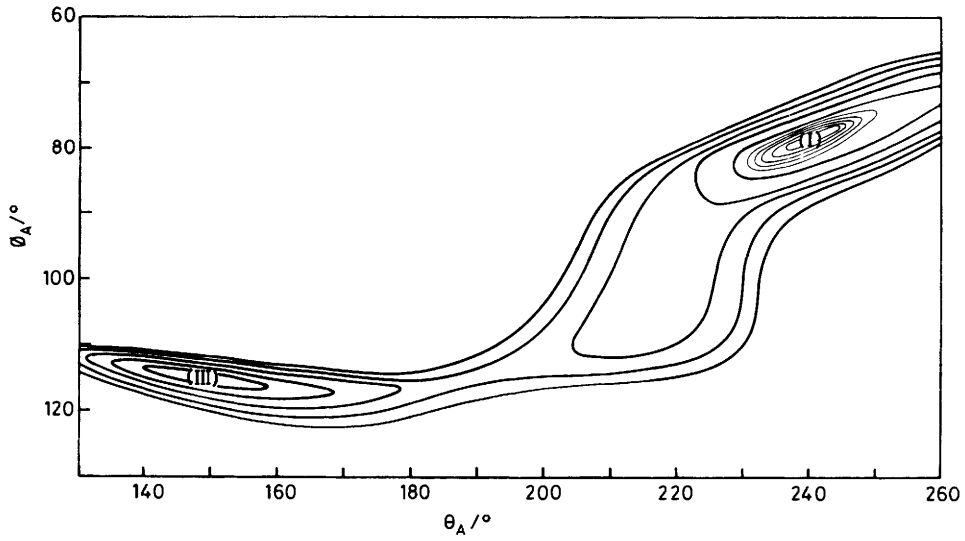

Figure 11. Projection of the potential-energy surface for [M(bidentate ligand)$_5$] onto the φ_A–θ_A plane. The five faint contour lines are for successive 0.02 increments above the minimum and the five heavy contour lines for successive 0.2 increments above the minimum; $n = 6$, $b = 1.20$. The positions of isomers (I) and (III) are shown

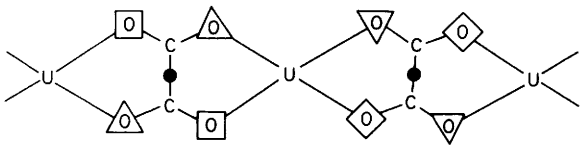

Figure 12. Polymerization in the triclinic phase *via* a succession of inversion centres along *a*; □, △, ◇, and ▽ denote symmetry-related sets of oxygen atoms. The inversion centres are denoted by ●

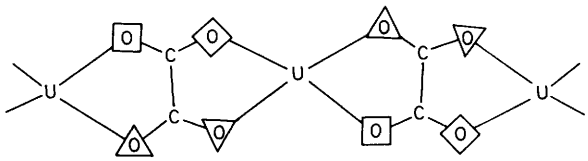

Figure 13. Polymerization in the orthorhombic phase *via* a two-fold screw along *b*; □, ◇, ▽, and △ denote the symmetry-related oxygen atoms

tral metal atom, is less than 3.3°. In general, the displacement from the minimum on the potential-energy surface is along the valley from stereochemistry (I) towards stereochemistry (II).

The only mononuclear compound in which the isomer (II) structure is observed is the barium diacetamide complex. The normalised bite of 0.98 is within the expected range for this stereochemistry (Figure 6). The triclinic phase of $K_4[Th(C_2O_4)_4]\cdot 4H_2O$ is isostructural with the triclinic form of $K_4[U(C_2O_4)_4]\cdot 4H_2O$, and both of these structures agree quite well with prediction, in spite of being polymeric. The orthorhombic form of $K_4[U(C_2O_4)_4]\cdot 4H_2O$ has a stereochemistry intermediate between that of isomers (II) and (III) (Figures 8 and 9). The bridging oxalate groups in these polymers are along the CD and C′D′ edges, and it can be seen from Figures 8 and 9 that the major difference between the bicapped square antiprism in isomer (II) and the sphenocorona in isomer (III) is that these CD and C′D′ edges are coplanar in the latter case. The polymer in the triclinic phase is generated by a succession of inversion centres along *a*, located at the mid-points of the bridging oxalate C–C bonds (Figure 12) and hence there are no crystallographic constraints on the relative orientation of the CD and C′D′ edges of the polyhedron. In the orthorhombic case the polymer is generated by a two-fold screw axis along *b* (Figure 13) and, given the near planarity of the oxalate ligands, this constrains the CD and C′D′ edges to be almost coplanar and distorts the stereochemistry away from a bicapped square antiprism towards a sphenocorona.

References

1 Part 4, D. L. Kepert, J. M. Patrick, and A. H. White, preceding paper.
2 B. Kojić-Prodić, Ž. Ružić-Toroš, and M. Šlujkič, *Acta Crystallogr., Sect. B*, 1978, **34**, 2001.
3 D. Tranqui, P. Boyer, J. Laugier, and P. Vulliet, *Acta Crystallogr., Sect, B*, 1977, **33**, 3126.
4 G. L. Glen, J. V. Silverton, and J. L. Hoard, *Inorg. Chem.*, 1963, **2**, 250.
5 M. N. Akhtar and A. J. Smith, *Acta Crystallogr., Sect. B*, 1975, **31**, 1361.
6 M. C. Favas and D. L. Kepert, *Prog. Inorg. Chem.*, 1981, **28**, 309.
7 D. L. Kepert, J. M. Patrick, and A. H. White, *J. Chem. Soc., Dalton Trans.*, 1983, 381.
8 D. L. Kepert, 'Inorganic Stereochemistry,' Springer, Berlin, Heidelberg, New York, 1981.
9 Y. C. Lin and D. E. Williams, *Can. J. Chem.*, 1973, **51**, 312.
10 B. E. Robertson, *Inorg. Chem.*, 1977, **16**, 2735.

Received 6th August 1982; *Paper* 2/1376